Paste 2024 – AB Fourie & D Reid (eds)
© 2024 Australian Centre for Geomechanics, Perth, ISBN 978-0-6450938-8-9
doi:10.36487/ACG_repo/2455_29

Calibration of the PM4Silt model for polymetallic fine grained mine tailings based on laboratory testing results

NG Bellido *Ausenco Peru SRL, Peru*

PG Mendoza *Ausenco Peru SRL, Peru*

Abstract

The seismic response of the tailing dams is highly dependent on the seismic response of the mine tailings to be stored and given the recent failures of tailings storage facilities around the globe, it is essential to understand the mechanical behaviour of different mine tailings. This paper presents a geotechnical characterisation of thickened tailings from polymetallic deposits, composed mainly of lead, silver, zinc and gold. The laboratory tests have been performed on tailings samples obtained from the tailings storage. The geotechnical characterisation has been developed based on results from special laboratory tests, such as cyclic direct simple shear, static triaxial, resonant column, and torsional shear. Cyclic direct simple shear and static triaxial tests have shown that the contractive tailings are susceptible to liquefaction, and that their behaviour is similar to low plasticity silts and clays. The results from cyclic tests show flatter liquefaction resistance curves compared to sands, these observations seem consistent with what has been observed on natural silts and few previous studies on mine tailings. In order to model the behaviour of tailings in dynamic simulations, the PM4Silt constitutive model is calibrated based on the laboratory test presented here. The calibrated model can reproduce reasonably well the cyclic strength curves measured in the laboratory at different confining pressures. The results indicate that the PM4Silt model can be used to simulate the cyclic behaviour of thickened tailings.

Keywords: *thickened tailings, polymetallic deposits, PM4Silt constitutive model, cyclic test*

1 Introduction

Currently, there are studies that have focused on the geotechnical characterisation of mining tailings through static and cyclic tests (e.g. Macedo & Vergaray 2022; Macedo et al. 2023; Vergaray et al. 2023), which provide trends of these materials. It is mentioned that the behaviour they exhibit is different from what is commonly observed in natural soils. These differences are attributed to the microstructure and mineralogy of mine tailings.

Due to recent failure of tailings storage facilities (TSFs) around the world and considering several thickened tailings storage facilities are located in the South American Andes in an area with high seismicity, it is essential to assess the cyclic behaviour of mine tailings.

This study presents a geotechnical characterisation of thickened tailings from a TSF located in the Peruvian Andes, with an emphasis on cyclic behaviour. The tailings were generated from polymetallic deposits, composed mainly of lead, silver, zinc and gold. This characterisation has been developed based on results from special laboratory tests such as cyclic direct simple shear, static triaxial, resonant column, and torsional shear on samples obtained from tailings storage. Furthermore, considering the current use of numerical tools for nonlinear dynamic analyses (NDAs) of tailing dams, the calibration of the constitutive model PM4Silt (Boulanger & Ziotopoulou 2019) for thickened tailings is presented. This model was developed for representing clays and plastic silts in NDAs, and recently employed to represent tailings (e.g. Macedo et al. 2022; Cerna-Diaz et al. 2023; Salam et al. 2021).

2 Geotechnical characterisation

The geotechnical characterisation program included static monotonous and cyclic test. Several samples were also recovered from test pits, which were used to characterise index properties and perform laboratory test. The index and particle distribution properties for the representative gradation are summarised in Table 1.

Table 1 Index properties of tailings

Material	Thickened tailings
Plasticity index (PI)	6 to 9%
Fine contents (FC)	44 to 51%
Specific gravity (Gs)	2.81 to 2.96
Unified soil classification system	SC-SM to CL

2.1 Monotonic loading behaviour

The specimens tested in monotonous triaxial compression tests showed plastic contractive behaviour under undrained conditions. The stress path curves (Figure 1a) lead to a constant volume friction angle (ϕ'_{cv}) of about 33°, corresponding to 20–25% of axial strain (ε_a) and its corresponding critical state stress ratio (M_{tc}) of about 1.33, within the range identified by Macedo & Vergaray (2022).

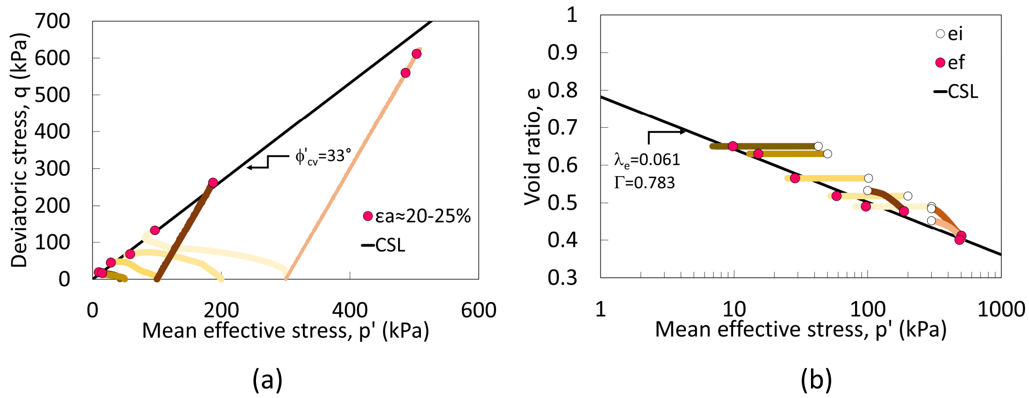

Figure 1 (a) Stress paths for monotonic drained and undrained triaxial tests; (b) Critical state line (CSL), with results from triaxial monotonic test on thickened tailings

The stress parameters are defined as follows:

$$p' = (\sigma'_1 + 2 \times \sigma'_3)/3 \quad (1)$$

$$q = \sigma'_1 - \sigma'_3 \quad (2)$$

where σ'_1 and σ'_3 are the major and minor effective principal stresses, respectively.

The results of drained and undrained monotonic triaxial tests (CD and CU, respectively) were used to produce the critical state line (CSL) indicated in the Figure 1b. Furthermore, it can be observed in the initial void ratio (ei) and in the critical state (ef).

According to the critical state soil mechanics framework, the CSL is defined as:

$$e_{cs} = \Gamma - \lambda_e \times \ln(p') \quad (3)$$

where in the case of a linear CSL:

Γ = altitude at 1 kPa

λ_e = slope.

2.2 Cyclic loading behaviour

2.2.1 Cyclic material properties

Resonant column and torsional shear (RCTS) tests were performed on disturbed samples. The specimens were placed in a resonant columns device and tested for the low amplitude shear modulus (G_{max}) and the low amplitude damping ratio as well as the variations of the shear modulus (G) and the damping ratio (ξ) with the shear strain. Figure 2 shows the RCTS results at different confining stresses, for this dual axis graph, the descending values correspond to the normalised shear modulus (G/G_{max}), and the ascending values correspond to damping ratio (ξ).

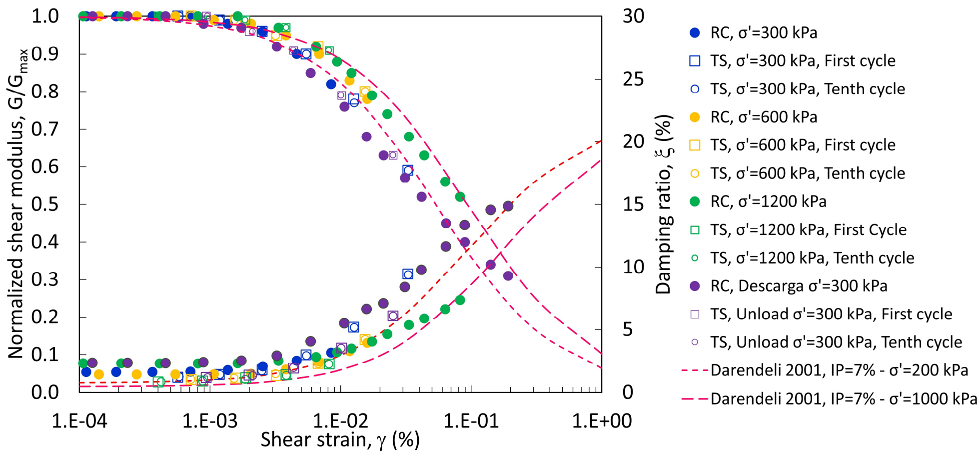

Figure 2 Normalised shear modulus and damping curves for the tested materials along with the curves from Darendeli (2001)

The results show that a given shear strain, G increases, and the damping ratio decreases with increasing confinement. The results were used to fit the G_{max} experimental data to the functional form in Equation 4.

$$G_{max} = G_o \times P_A \times (\sigma'/P_A)^{n_G} \tag{4}$$

where:

G_o and n_G	=	fitting parameters that depend on the material
σ'	=	isotropic confining effective stress
P_A	=	atmospheric pressure (101.3 kPa).

Figure 3a shows the variation of shear modulus with the shear strain (same colour legend as Figure 2) and Figure 3b the maximum shear modulus with the mean effective stress.

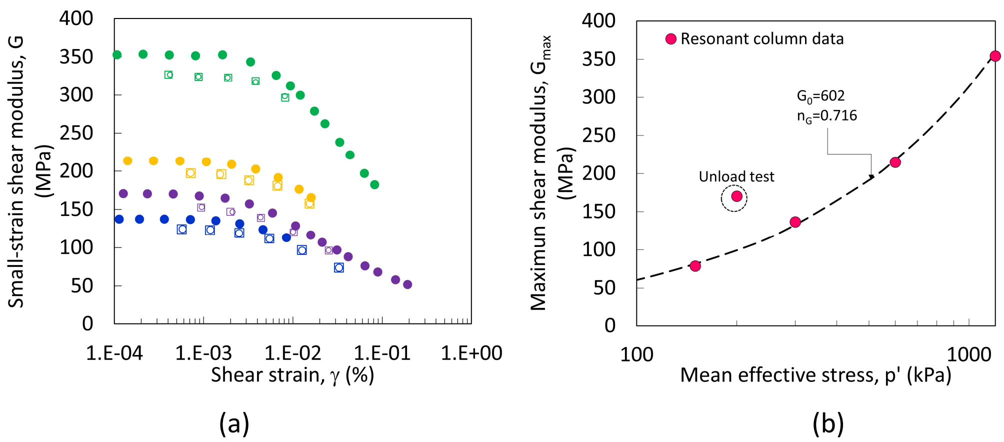

Figure 3 (a) Small-strain shear modulus versus shear strain; (b) Maximum shear modulus data for materials

2.2.2 *Cyclic simple shear test and liquefaction resistance*

Cycle simple shear (CSS) tests were also performed to investigates the cyclic response and liquefaction resistance curves of the thickened tailings. The sample was sheared under a harmonic sinusoidal loading at 0.05 Hz, with amplitude characterised by a defined cyclic stress ratio (CSR) (which is the ratio of the cyclic shear stress to the initial vertical effective stress). Figure 4 shows the response observed during the CSS test.

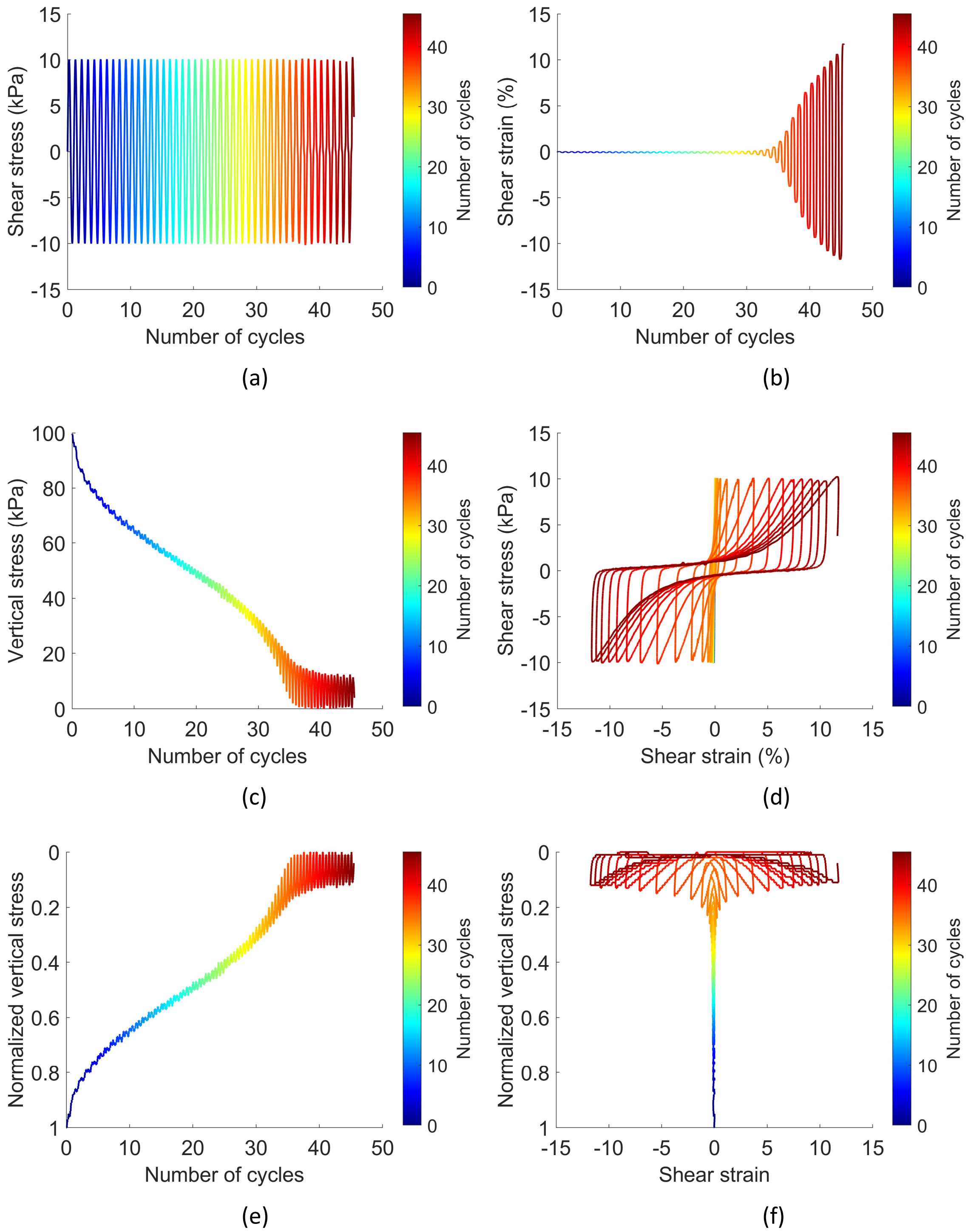

Figure 4 Results of a cyclic simple shear (CSS) test for CSR=0.10 at 100 kPa and α=0.0 (initial static shear stress) a) shear stress versus no. of cycles; b) shear strain versus no. of cycles; (c) vertical stress versus no. of cycles; d) shear stress versus shear strain; e) normalised vertical stress versus no. of cycles; f) normalised vertical stress versus shear strain

A deformation criterion based on 3.75% single amplitude was chosen to identify the occurrence of liquefaction. Figure 5 shows the number of cycles to the 'liquefaction' criterion plotted against the applied CSR for all the CSS test performed in this study. In concordance with Macedo et al. (2022), the slopes of the liquefaction resistance curves for tailings are flatter than typical curves for sands. It was observed that the liquefaction resistance curves do not present an important sensitivity in terms of the confinement stress before the cyclic loading, which contrasts with sands behaviour (Idriss & Boulanger 2008).

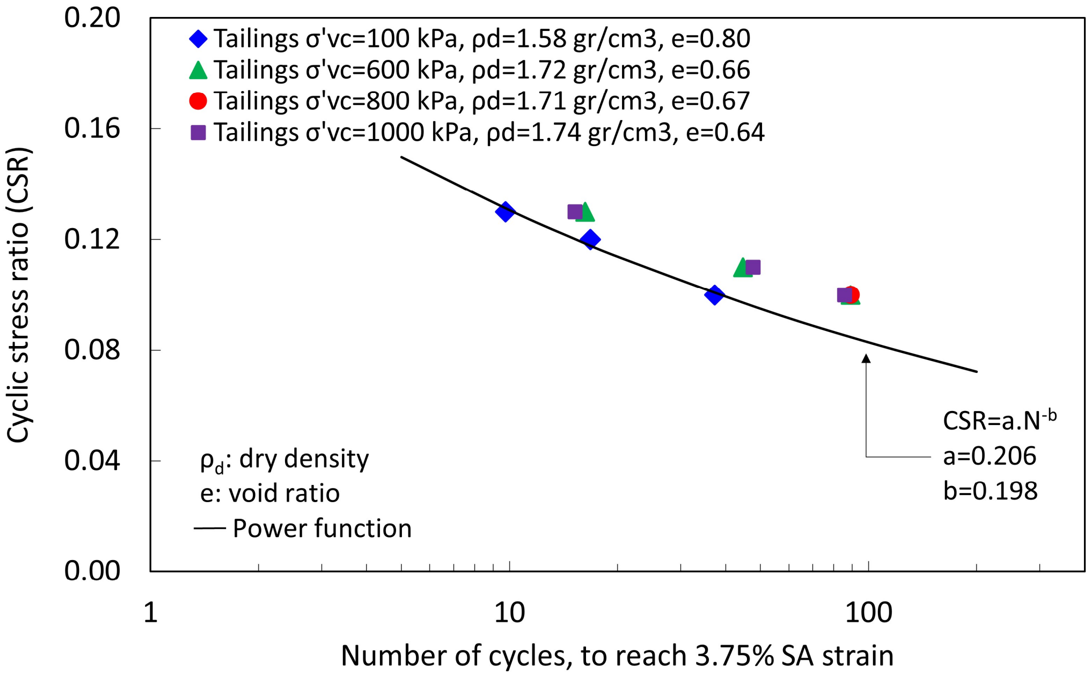

Figure 5 Liquefaction resistance curve for thickened tailings at different confining stress

3 Calibration of PM4Silt parameters

PM4Silt is an effective stress-based bounding surface plasticity model formulated to model the dynamic behaviour of low plasticity silts and clays (Boulanger & Ziotopoulou 2023). The model utilises the same general framework as the PM4Sand constitutive model, but the formulation is modified to better represent undrained behaviour of silts and clays instead of cohesionless granular soils.

The model is limited to plane strain applications and cannot represent strength anisotropy. PM4Silt is not recommended for applications involving consolidation processes as the model does not include a cap on yield surface. More detailed information on the model formulation and implementation is available in Boulanger & Ziotopoulou (2023).

Calibration of the PM4Silt constitutive model is performed using the single element DSS drivers as recommended by Boulanger & Ziotopoulou (2023). Strain controlled undrained cyclic DSS drivers are used to calibrate for shear modulus reduction and equivalent damping ratio behaviour using relationships presented by Darendeli (2001). Stress ratio (shear stress normalised by vertical effective stress) controlled undrained cyclic DSS drivers are used to calibrate the thickened tailings to target CSR required to cause 3.75% strain.

The primary input parameters of the PM4Silt constitutive model are the undrained shear strength ratio ($S_{u,cs}/\sigma'_{vc}$) (or undrained shear strength $S_{u,cs}$), the shear modulus coefficient (G_o), the contraction rate parameter (h_{po}), and an optional post-strong shaking shear strength reduction factor. The secondary input parameters of the model have default values. Still, they can be set according to the available information for the material being evaluated using information from CSS test and liquefaction resistance curve.

To calibrate the PM4Silt model, $S_{u,cs}/\sigma'_{vc}$ was estimated from monotonic undrained triaxial tests. G_o and shear modulus exponent (n_G) values were calculated from the RCTS tests. Critical state friction angle (ϕ_{cv}) and λ were obtained from the CSL, all remaining parameters except h_{po} were initially assigned default parameters as Boulanger & Ziotopoulou (2023) recommended. Undrained cyclic loading simulations with uniform CSR were performed in FLAC (Itasca Consulting Group 2019) to calibrate h_{po} using the experimental liquefaction resistance curves as target. The stress–strain and stress path responses in the experimental and numerical simulations are examined to further modify secondary parameters. The secondary parameters were modified to flatten the liquefaction resistance curve and generate stress–strain and excess pore pressure responses similar to those observed experimentally. The summary of the calibrated PM4Silt parameters is presented in the Table 2.

Table 2 Input parameter for PM4Silt calibration for thickened tailings

Input parameters		Default value	Calibration parameters
Primary parameters			
Undrained shear strength ratio at critical state	$S_{u,cs}/\sigma'_{vc}$	–	0.134
Shear modulus coefficient	G_o	–	602
Contraction rate parameter	h_{po}	–	8
Secondary parameters			
Initial void ratio	e_o	0.9	0.8
Shear modulus exponent	n_G	0.75	0.716
Critical state friction angle	φ_{cv}	32	33
Compressibility in e-ln(p') space	λ	0.06	0.061
Sets bounding p_{min}	$r_{u,max}$	$p_{min}=p_{cs}/8$	0.98
Bounding surface parameter	$n^{b,wet}$	0.8	Default
Bounding surface parameter	$n^{b,dry}$	0.5	Default
Dilation surface parameter	n^d	0.3	Default
Dilatancy parameter	A_{do}	0.8	Default
Plastic modulus ratio	h_o	0.5	Default
Fabric term	z_{max}	$10 \le 40(S_u/\sigma'_{vc}) \le 20$	Default
Fabric growth parameter	c_z	100	Default
Strain accumulation factor	c_ξ	$0.5 \le (1.2S_u/\sigma'_{vc}+0.2) \le 1.3$	Default
Modulus degradation factor	C_{GD}	3	Default
Plastic modulus factor	$C_{k\alpha f}$	4	Default

Figure 6 shows the ability of PM4Silt model to capture undrained cyclic behaviour of thickened tailings. Furthermore, PM4Silt show successfully captured the key cyclic behaviour in terms of cyclic strain accumulation and pore pressure generation. Also shown on this figure are the modulus reduction and equivalent damping ratio obtained from single element simulations of undrained DSS loading at different strain amplitudes under a range of consolidation stress and the relationships recommended by Darendeli (2001). The equivalent damping ratios for PM4Silt are greater than either empirical correlation, which is a common limitation for this type of model (Boulanger 2019).

Figure 7 shows the derived PM4Silt based cyclic resistance curves calibration against laboratory cyclic direct simple shear (CDSS) for a cyclic strain of 3.75% at 100 kPa. As evidenced in the figure, for confinement stresses between 600 and 1,000 kPa, additional calibration parameters might be necessary. These parameters could ultimately be employed in NDAs by discretising the behaviour based on confinement stress.

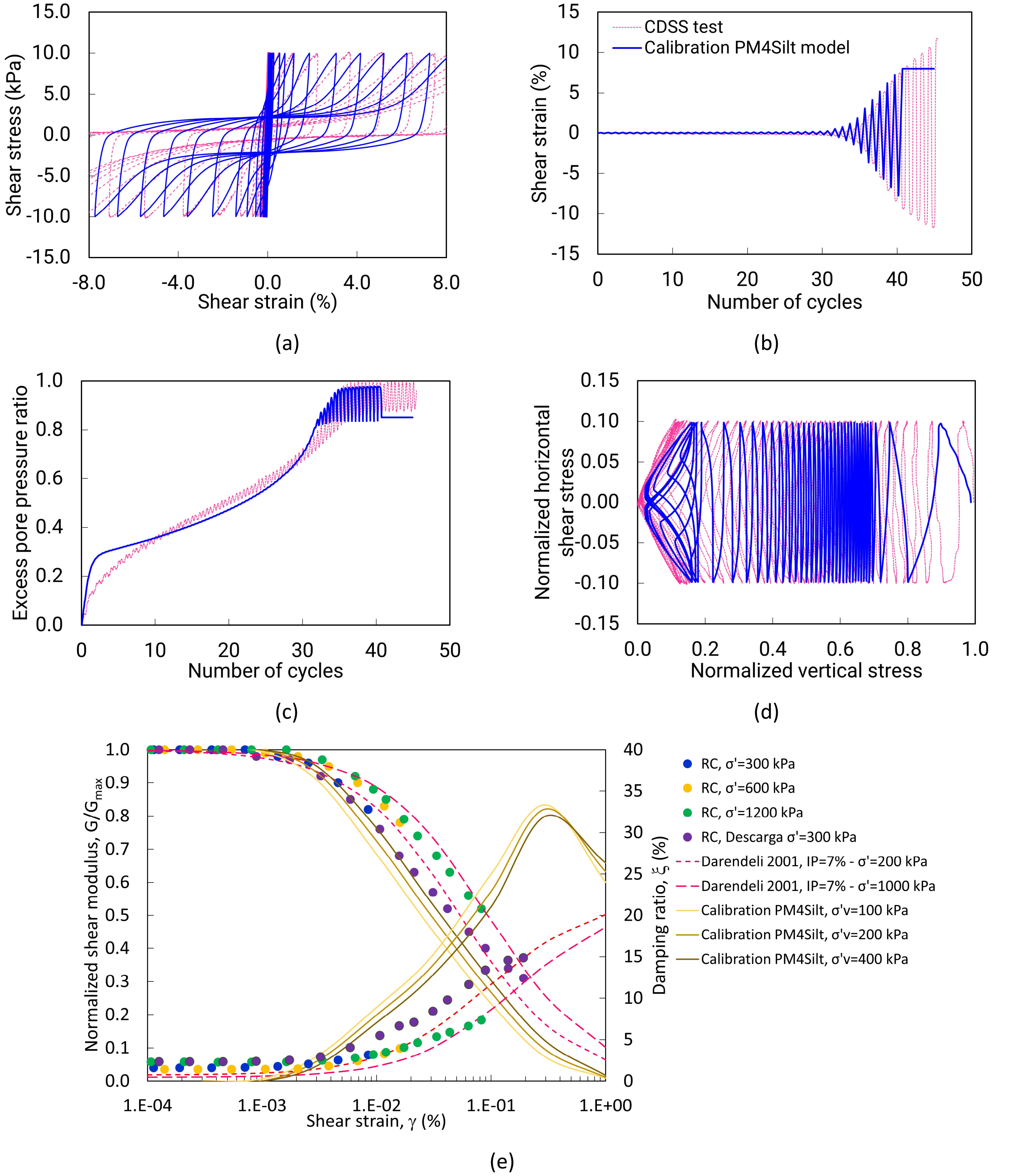

Figure 6 PM4Silt single element simulations for CSR=0.10 at 100 kPa and α=0.0 (a) Cyclic stress versus shear strain; (b) Shear strain versus no. of cycles; (c) Excess pore pressure ratio (R_u) versus no. of cycles; (d) Normalised shear stress versus normalised vertical stress; (e) Shear modulus reduction versus shear strain amplitude and equivalent damping ratio versus shear strain amplitude

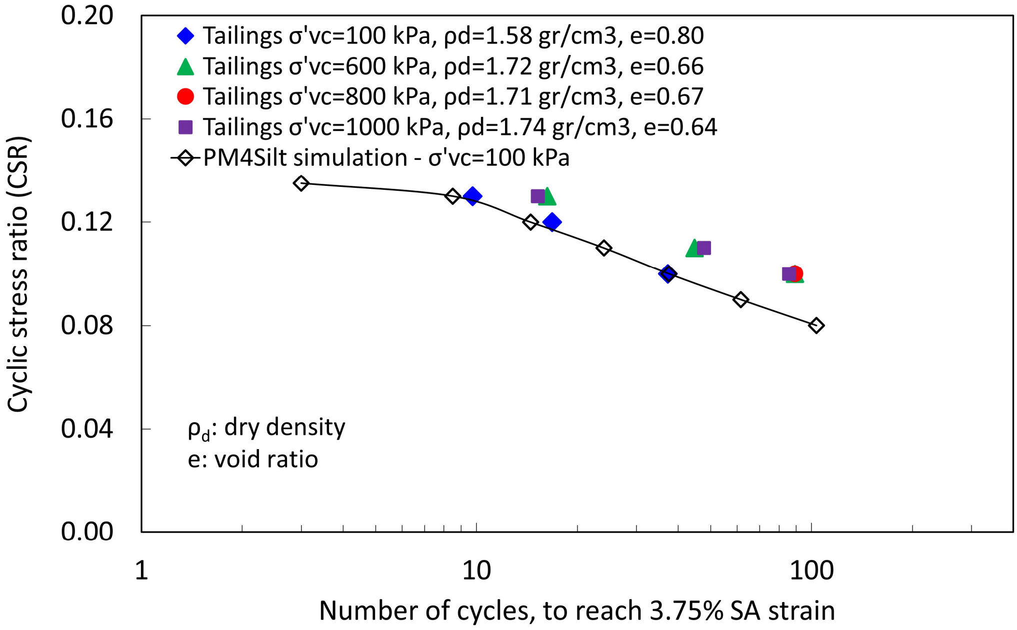

Figure 7 Simulation of liquefaction resistance curve for the confinement of 100 kPa

4 Conclusion

In this study, the PM4Silt model parameters were determined for thickened tailings based on laboratory tests. Drained and undrained monotonic triaxial tests were used together to generate the critical state line. RCTS tests were used to estimate the maximum shear modulus according to the confining pressure, the variations of the shear modulus and the damping ratio with the shear strain. CDSS tests were used to determine the liquefaction resistance curves, stress–strain, stress path, and excess pore pressure responses.

The PM4Silt model produced simulated responses that were reasonably consistent with the available laboratory tests, such as, cyclic loading behaviour important to many earthquake engineering applications (e.g. NDAs).

The calibrated model is valid for the thickened tailings considered in this study; additional adjustments may be required when using the model for other tailings. Additionally, the calibration presented here could be updated based on field testing results for its application in NDAs.

Acknowledgement

The authors would like to acknowledge the support of the Ausenco Lima office for providing the laboratory tests analysed in this study.

References

Boulanger, RW 2019, 'Nonlinear dynamic analyses of Austrian dam in the 1989 Loma Prieta earthquake', *Journal of Geotechnical and Geoenvironmental Engineering*, vol. 145, no. 11, https://doi.org/10.1061/(ASCE)GT.1943-5606.0002156

Boulanger, RW & Ziotopoulou, K 2019, 'A constitutive model for clays and plastic silts in plane-strain earthquake engineering applications', *Soil Dynamics and Earthquake Engineering*, vol. 127, p. 105832, https://doi.org/10.1016/j.soildyn.2019.105832

Boulanger, RW & Ziotopoulou, K 2023, *PM4Silt (Version 2.1): A Silt Plasticity Model for Earthquake Engineering Applications*, Center for Geotechnical Modeling, Department of Civil and Environmental Engineering, University of California, Davis.

Cerna-Diaz, A, Kafash, M, Davidson, R, Yenne, L & Doughty, P 2023, 'Nonlinear deformation analyses of a tailings dam during a Mw5.7 earthquake', *Geo-Congress 2023: Geotechnical Systems from Pore-Scale to City-Scale*, VA, American Society of Civil Engineers, Reston, pp. 70–85, https://doi.org/10.1061/9780784484708.007

Darendeli, MB 2001, *Development of a New Family of Normalized Modulus Reduction and Material Damping Curves*, PhD thesis, The University of Texas at Austin, Austin.

Idriss, IM & Boulanger, RW 2008, *Soil Liquefaction During Earthquakes,* Earthquake Engineering Research Institute, Oakland.

Itasca Consulting Group 2019, *FLAC – Fast Lagrangian Analysis of Continua*, computer software, version 8.1.

Macedo, J, Sotelo, G, Orellana, S, Vergaray, L, Liu, F, Jaffal, H & El Mohtar, C 2023, 'Geotechnical characterization of collapsible salty sands subjected to monotonic and cyclic loadings – A case study for areas with high seismicity', *Soils and Foundations*, vol. 63, issue 1, p. 101252, https://doi.org/10.1016/j.sandf.2022.101252

Macedo, J, Torres, P, Vergaray, L, Paihua, S & Arnold, C 2022, 'Dynamic effective stress analysis of a centreline tailings dam under subduction earthquakes', *Proceedings of the Institution of Civil Engineers - Geotechnical Engineering*, vol. 175, issue 2, pp. 224–246, https://doi.org/10.1680/jgeen.21.00017a

Macedo, J & Vergaray, L 2022, 'Properties of mine tailings for static liquefaction assessment', *Canadian Geotechnical Journal*, vol. 59, pp. 667–687. https://doi.org/10.1139/cgj-2020-0600

Salam, S, Xiao, M, Khosravifar, A & Ziotopoulou, K 2021, 'Seismic stability of coal tailings dams with spatially variable and liquefiable coal tailings using pore pressure plasticity models', *Computers and Geotechnics*, vol. 132, p. 104017, https://doi.org/10.1016/j.compgeo.2021.104017

Vergaray, L, Macedo, J & Arnold, C 2023, 'Static and cyclic liquefaction of copper mine tailings', *Journal of Geotechnical and Geoenvironmental Engineering*, vol. 149, no. 5, https://doi.org/10.1061/JGGEFK.GTENG-10661